Adsorption of Lead onto a Waste Biomaterial-Biochar

Yasser A. El-Damarawy[1], Maher E. Saleh[2#], Faiz F. Assaad[1], Abel-Salam A. Abdel-Salam[2], Refat A. Youssef[1]

[1.] Soils and Water Use Department, National Research Centre, Cairo, Egypt; [2.] Department of Soils and Water Sciences, Faculty of Agriculture, Alexandria University, postal code 21545 El-Shatby, Alexandria, Egypt.
Corresponding author: maher.saleh@alexu.edu.eg

Abstract: Sugarcane bagasse biochar (SCBB) as a waste bio-adsorbent material was obtained using slaw pyrolysis (at 500^oC and 30 min residence time and limited oxygen conditions) for its feedstock. The resulted biochar had a recalcitrant features, total surface area 175.4 m^2g^{-1}, total pore volume (p/p^0) 0.11 $cm^3 g^{-1}$, and CEC 86.96 $mmol.kg^{-1}$. The adsorption capacity of the SCBB for lead ions (Pb^{2+}) was studied at different initial Pb^{2+} solution concentrations (0.1 – 1.5 mM) in the form of lead nitrate. The maximum adsorption of Pb^{2+} was obtained at initial concentration 0.1 mM and the adsorption of Pb^{2+} attained equilibrium at about 15 min, with maximum removal percent of 97.0%. Pb^{2+} removal efficiency decreased gradually with the increase of initial metal concentration. Lead adsorption capacity increased with the increase of its concentration and almost a constant value was achieved at higher concentration. Adsorption of lead ions on the biochar was studied with various adsorption isotherm models such as Langmuir, Freundlich, Temkin, and Dubinin-Radushkevich. The equilibrium adsorption data was better fitted to Langmuir isotherm ($R^2 =0.9985$). Kinetic modeling of Pb^{2+} was also studied by using Pseudo first and second orders, Intra-Particle Diffusion and Boyd Model. The adsorption kinetic data was better fitted to the Pseudo second order model for all tested concentrations (R^2 ranged from 1.0 to 0.998).

1-Introduction

Due to the nature and quantity of the metal ingested, heavy metals can cause serious health problems (Adepoju-Bello and Alabi, 2005). It is vital to inform ourselves about the heavy metals and to take protective measures against excessive exposure. In aquatic system, heavy metals can be found in different forms, whereby influencing their toxicity for bio-organisms, including free ions organic and inorganic complexes, precipitates, mineral particles, and metals present in biota. Lead for instance is a commutative poison and a possible human carcinogen and it is well known for its direct, destructive effect on neuronal function (Bakare-Odunola, 2005). Also lead has direct adverse effect on cells in the arterial wall. The most resources of lead in our aquatic system come from drainage and surface runoffs effluent discharges from industries.

Most of the treatment processes that have been used to remove heavy metals from wastewater include precipitation, coagulation, ion exchange, electrodialysis, membrane filtration, flotation, reverse osmosis, and adsorption are suffering from high cost and difficult to implement on a large scale. The use of biochar as a low-cost waste sorbent to remove heavy metals contaminants from aqueous solutions is an developing (evolving) and talented wastewater treatment technology, which has already been established in various studies.

Biochar usually has adsorption ability for heavy metals due to its greater surface area, negative surface charge, and charge density (Dong et al., 2011; Gan et al., 2015; Liang et al., 2006; Saleh et al., 2016). Thus, the use of biochar to remediate the wastewater from its heavy metals pollutants offers a potential environmental benefit by protecting our water resources. The aim of this work is to study lead removals from synthetic wastewater by using sugar cane bagasse as a bio-adsorbed material.

2-Materials and Methods

The waste raw material of sugar cane bagasse (SCB) was washed several times by distilled water (pH 7) to remove irrelevant materials such as dirt, sand and other impurities. The residues were divided into smaller particle sizes. The cleaned materials were dried at 70^oC for 48 h then stored in air-tight plastic jars prior the pyrolysis process.

To prepare biochar material, the residues material (feedstock) was converted into biochar through slow pyrolysis at 500 C^o for 30 min in absence of oxygen environment in a muffle furnace (VULCANE A-550). The feedstock was placed in a ceramic vessel and covered to avoid air contact, following the procedures described by Mahmoud et al., (2011). After cooling,

the sugar cane bagasse biochar (SCBB) was kept in desiccators. The yield percentage of biochar was calculated. The biochar was then ground and sieved through plastic sieve to obtain the less than 0.5 mm sized particles. After several rinses with deionized water (to remove impurities such as ash), the biochar dried at 80 C^o for 48 hours and stored in plastic jars for further tests.

Stock solution of 30 mmol L^{-1} lead (II) as nitrate was prepared by dissolving appropriate amounts of Pb $(NO_3)_2$ (Merck Co.) using deionized water. All solutions were arranged by a proper dilution from the stock solution with deionized water. Solutions of 0.01M KCl were used as a background in different electrolyte for all the adsorption experiments.

2.1 Biochar Characterizations:

Some of the biochar characterizations were done by using the standard methods and techniques. Yield percentage, ash content, moisture content, pH by using (pH-meter Inolab pH/Ion 735), elemental analysis: Carbon, Hydrogen, and Nitrogen contents by using (Vairo type, El, elemental analyzer), heavy metals by using atomic absorption spectrophotometer (Varian, spectra AA Model 220), CEC (Sumner and Miller, 1996) and surface area was determined using N_2 sorption isotherms run on Surface area meter (BELSORP - mini II). Scanning electron microscopy (SEM) coupled with energy dispersive spectroscopy (EDAX) (QUANTA FEG 250 with an Oxford EDS) was used to examine the surface morphology and surface functional groups analysis (FTIR – 6100 JASCO spectrometer in the range 4000–400 cm^{-1}) was done according to standard methodologies.

2.2 Adsorption Experiment:

Batch adsorption experiments were carried out in a series of reaction vessels. 5.0 gm SCBB samples as adsorbent were added into the reaction vessels with 1000 ml aqueous solution of lead in the presence of 0.01M KCl solution as a background electrolyte. Suspensions were continuously stirred at 400 rpm and the reaction were conducted at temperature of 25^oC for 24 hours, during the reaction 20 ml aliquots of suspension were withdrawal from the reaction vessel at different times intervals 5, 10, 15, 30 minute, 1, 2, 4, 6, 12 and 24 hours with a polyethylene syringe. The pH was measured in that suspension and then filtered immediately. The Pb concentrations in the filtrates were determined using AAS Varian spectra AA Model 220 using air-acetylene flame.

The amount of Pb ions adsorbed in mmol per gram was determined by using the following mass balance equation (1):

$$m_A (q) = V (C_o - C)\dots\dots\dots\dots\dots\dots (1)$$

Where:

m_A: mass of biochar (g);

V: volume of solution (L);

C: concentration after adsorption (mmol L^{-1});

C_o: initial concentration (mmol L^{-1});

q: amount adsorbed (mmol g^{-1} of biochar).

Percentage removal of Pb ions was calculated by equation (2):

$$\text{Removal \%} = 100 (C_o - C)/ C_o\dots\dots\dots\dots (2)$$

3. Results and discussion:

3.1 Surface properties of SCBB:

The elemental analysis of the biochar showed that hydrogen content was high in the biochar. The predominant elemental component was carbon. The percentage of oxygen-containing groups was 35.08% with higher N and S contents (Table 1). These may contribute on the complication and precipitation of lead. The O/C ratio of SCBB was 0.55 and pointed to its polar group content (Chen et al., 2008). Table (2) presents the main physical and electrical properties of the biochar. Physicochemical properties of biochars, such as pH, surface potential, and surface area, are important factors controlling their environmental applications (Inyang et al., 2010). On the other hand, the FTIR spectrum of SCBB before lead adsorption revealed a large number of absorption peaks within the interval of 4000–400 cm^{-1}, which is a sign of the complex chemical nature of SCBB.

Table1. Elemental analysis of Sugar cane bagasse biochar (SCBB) used in the lead (Pb) removal study.

Parameter	Values
pH	4.85
C %	63.50
H %	0.68
N %	0.688
S %	0.058
O %	35.08
molar ratio	
H/C	0.011
O/C	0.552
(O + N)/C	0.22
Heavy metals (mg kg^{-1})	
Pb	3.00
Ni	8.90
Cu	16.00
Cd	0.66

Table 2. The main physical and electrical properties of the sugarcane bagasse biochar (SCBB) used in the study.

Property	Value
Surface area ($m^2 g^{-1}$)	175.4
Total pore volume ($cm^3 g^{-1}$)	11×10^{-2}
Mean pore diameter (nm)	2.5351
Cation exchange capacity (mmol kg^{-1})	86.96
Surface charge density (esu[#])	1.44×10^5
Area per monovalent charge ($Å^2$)	33.49

#: esu: electro-static units

The scanning electron microscope (SEM) images showed the highly porous structure of the SCBB (Figure 2). The biochars' structure consisted of a highly complex network of pores. The images of biochar before and after adsorption are shown to illustrate the physical changes to the surface morphology of biochar following adsorption. Figure (1) shows that the SCBB possessed uniform pores and smooth wall surfaces under 5000x magnification. It can be seen that the pores on biochar have similar size with maximal diameter of 10 μm. There are significant changes to the surface morphology of the biosorbents before and after Pb^{2+} adsorption, as well as the formation of discrete aggregates on their surfaces following metal ion adsorption.

3.2 Effect of initial metal concentration:

The effect of initial concentration on the sorption of Pb (II) ions was carried out with the concentrations of 0.1, 0.3, 0.5, 1.0 and 1.5 mmole L^{-1} at $25C^o$. A result for the adsorption of lead ions on SCBB was plotted between the amounts adsorbed (q_e) versus the initial concentration of metal in the solution (C_o) and were demonstrated in Figure (2). Lead ions removal efficiency decreased gradually with the increase of initial metal concentration. For instance, after 15 minute Pb (II) removal efficiency of 96.86% was observed at initial concentration of 0.1 mmol L^{-1}. A further increase in the initial concentrations of Pb (II) in solution led to a decrease in the adsorption efficiency to 94%, 77.93%, 56.18% and 39.27% for initial concentration levels of 0.1, 0.3, 0.5, 1.0 and 1.5 mmol L^{-1} respectively. This phenomenon was explained by the limited number of active sites on the surface of the adsorbent. At high-level concentrations, the available sites of adsorption become fewer. This behavior is connected with the competitive diffusion process of the ions through the micro channel and pores of the biochar (Al-Anber and Al-Anber 2008). This means, energetically less favorable sites will be produced by increasing metal concentration in aqueous solution. Metal ions were absorbed by specific sites at low concentrations, but the adsorbed amount did not increase proportionally for higher metal ion concentrations since the active sites were filled and saturated. Hence, it was very clear that the percentage removal of lead ions decreased with increase in its ions concentration (Sposito, 1984; Putra et al. 2014 and Park et.al. 2015) as shown in Fig. 2.

3.3 Effect of contact time:

The required contact time for adsorption to be completed is important to give insight into an adsorption process. This also affords evidences on the minimum time required for significant adsorption to take place, the potential diffusion control mechanism between the adsorbent and the adsorbate and also to

determine the adsorption kinetics of an adsorbate at its given initial concentration.
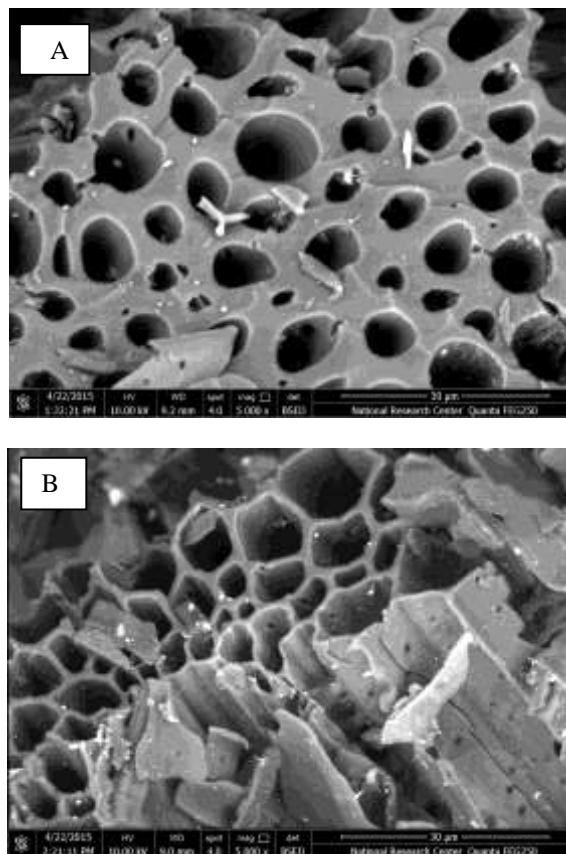
Figure 1. Scanning electron micrographs (SEM) of sugar cane bagasse biochar (SCBB) before (A) and after (B) the removal reactions of Pb^{2+} ions from aqueous solutions at 25°C
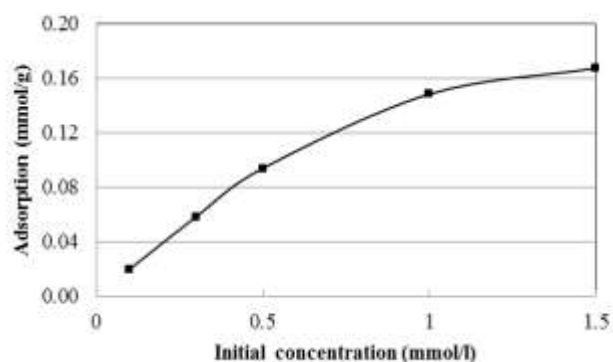
Figure 2. Removal of lead metal ions from aqueous solution by SCBB under different initial concentration at 25 C^o.

Results on the effect of contact time on the removal of lead ions (Pb^{2+}) are shown in Figures (3). These results indicated that with the increase of time the removal of Pb^{2+} increased to a certain point of

equilibrium. During the first fifteen minutes of the adsorption reaction, for example 96.86% of the total amount of Pb (II) was immobilized. The state of ion equilibrium in the biochar structure is reached after 96 hours. At that time, 98.99% was removed by SCBB at metal concentration of 0.1 mmol L^{-1}. Also by increasing the outside solution of Pb^{2+} from 0.1 to 1.5 mmol L^{-1}, the removal efficiency sequence was almost the same as in 0.1 mmol L^{-1} solutions.

This may be explicable as follows: the adsorbent sites eventually become saturated with adsorbed cations and then further addition of adsorptive ions would not be expected to increase the amount adsorbed significantly. With increase the time, the available sites of adsorption become fewer. This behavior is connected with the competitive diffusion process of the ions through the microchannel and pores. This competitive will lock the inlet of channel on the surface and prevents the metal ions to pass deeply inside the adsorbed material, *i.e.* the adsorption occurs on the surface only (Al-Anber and Al-Anber, 2008).

3.4 Adsorption of Lead

As Shown in Fig. 2, the maximum adsorption of lead on SCBB was 178.4 mmole kg^{-1}. Mohan, et al., (2007) and Shi et al., (2009) stated that high adsorption of Pb^{2+} from solution on adsorbents through surface electrostatic attraction could be attributed to its high electronegativity constant (-2.33), which results in a high tendency for specific adsorption. It is also usually attributed to its physical characteristics. For example, the hydrated radius of Pb^{2+} is small (4.01 Å); favoring columbic interactions of Pb with negative sites (Uchimiya et al., 2010).

Furthermore, Pb^{2+} has a greater affinity for most functional groups including carboxylic and phenolic groups, which are hard Lewis bases meanwhile lead is a hard Lewis acid. Moreover, lead has low pK_H (negative log of hydrolysis constant; 7.71). These factors favor Pb^{2+} for inner sphere surface sorption/ complexions reactions (Sposito, 1984).
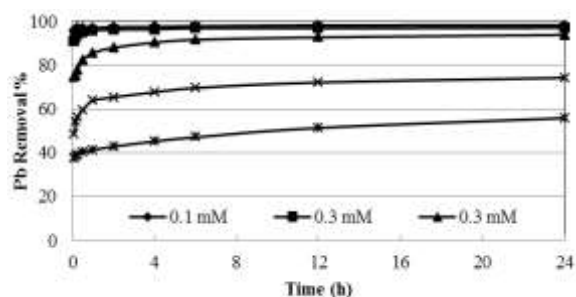
Figure 3. The effect of contact time and initial concentration on the removal % of Lead ions at 25 C^o.

According to pH of the biochar (pH = 4.95, Table 1), it can be assumed that metal ion in solution can able to bind chemically with carboxyl groups in the carbon. This means that an ion-exchange reaction takes place in the adsorption of lead ions. The ion-exchange reaction is accomplished through the substitution of protons of the surface carboxyl by meal ion, according to the following reaction (Khalid, et al. 1998).

$$M^{n+} + M(-COOH) \longleftrightarrow M(OOC-)_m^{n-m} + mH^+ ...(3)$$

Where: M^{n+} = metal ion with n^+ charge, -COOH = carboxyl group, and mH^+ = number of protons released. In such a system, at low pH, because of the high concentration of H^+, equation (3) lies to the left. The ion exchange sites are mainly protonated and are less available for ion exchange. Equation (3) proceeded further to the right and metal ion removal is increased by increased pH. Within this pH range, the ion exchange process is the major mechanism for removal of metal ion from solution.

The FTIR spectra before and after adsorption of 1.5 mmol L^{-1} Pb were used to examine the vibrational frequency changes in the functional groups. From FTIR study, the formation of new absorption bands, the change in absorption intensity, and the shift in wave number of functional groups could be due to interaction of metal ions with active sites of biosorbents. Results from this study suggested that carbonyl, hydroxyl and amine are the main adsorption sites in SCBB. Inyang et al. (2010) indicated that the active participation of –CO–, –OH, and –C–OH group in metal binding on biochars. Based on these observations, it can be stated that the functional groups (-OH, C-H, -CO, and C-OH) at these wave numbers have participated in lead adsorption on SCBB surfaces. Previous studies have shown that physicochemical properties of biochar, such as pH, surface potential, and surface area, are important factors controlling its environmental applications (Inyang et al., 2010). SCBB was acidic with a relatively low pH (4.95). The surface potential measurements (Table 2) indicated that SCBB has high negative surface charge which may be related to its higher surface area and pore volume. These data seems to suggest a greater potential for SCBB to sorb abundant positively charged heavy metals.

3.5 Adsorption isotherm

Heavy metal adsorption is usually modeled by the classical adsorption isotherms. In this study, four isotherms models Langmuir, Freundlich, Temkin and Dubinin-Radushkevich were used. At lower initial ion concentrations, the adsorption increased linearly while at higher concentrations, the adsorption did not increase proportionally due to the limited number of active sites on the adsorbent surfaces (Thilagan, et al., 2013).

3.5.1 Langmuir isotherm:

The Langmuir equation can be written in the following linear form:

$$C_e/q_e = 1/(q_{max}K_L) + C_e/q_{max} \dots\dots\dots\dots\dots\dots (4)$$
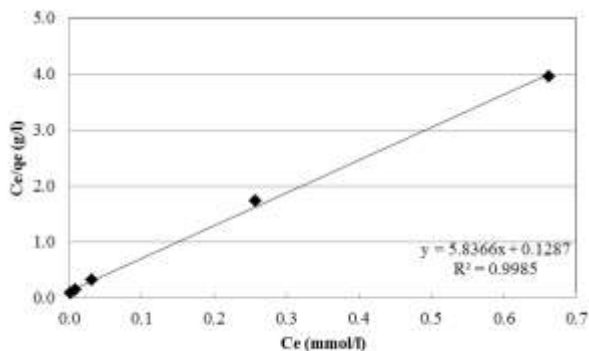
Figure 4. Langmuir isotherm plot for the adsorption of Pb^{+2} by SCBB at 25 C^o.

Where: C_e (mmol L^{-1}) is the concentration of the lead ions at equilibrium, q_e is the equilibrium adsorption capacity of the adsorbent (mmol kg^{-1}), K_L (L mmol^{-1}) is the Langmuir constant related to the adsorption energy and q_{max} (mmol g^{-1}) is the adsorption capacity were evaluated from the intercept and slope of the linear plot of experimental data (Table 3). The plots of C_e/q_e versus C_e are shown in Figures (4). The high K_L of Pb (II) suggested its high affinity towards the SCBB surface (Gupta et al., 2005). The essential characteristics of the Langmuir isotherm can be expressed in terms of the dimensionless separation parameter called the equilibrium parameter (R_L) which indicates the isotherm shape that predicts whether an adsorption system is favorable or unfavorable. RL is defined as:

$$R_L = 1/(1+ K_LC_o) \dots\dots\dots\dots\dots\dots\dots\dots. (5)$$

The R_L value indicates the type of isotherm. The adsorption is to be unfavorable ($R_L > 1$), linear ($R_L = 1$) and favorable ($R_L < 1$) (Arami et al., 2005). The R_L value obtained from the experimental data is much closer to zero indicating favorable adsorption for lead ions on the biochar. The R^2 of adsorption was very high indicating that Pb^2 on SCBB can be described by sing Langmuir isotherm.

Table 3. Isotherm model parameter of Pb sorption on SCBB at 25 C^o.

q_{max} actual (mmolkg^{-1})	Langmuir Isotherm			Freundlich Isotherm			Temkin Isotherm		
	q_{max} (mmolkg^{-1})	K_L (Lmmol^{-1})	R^2	K (mmol kg^{-1})	1/n	R^2	b (jmol^{-1})	A (Lkg^{-1})	R^2
178.4	171.33	45.35	0.999	234.75	0.341	0.916	98.25	1264	0.999

3.5.2 Freundlich isotherm:

The experimental data were analyzed by Freundlich isotherm model in its linearized form:

$$\log q_e = 1/n \log C_e + \log K_F \dots\dots\dots\dots\dots\dots (6)$$

Where: K_F is the Freundlich adsorption constant and it is the maximum adsorption capacity of metal ions (mmol kg^{-1}), C_e is the equilibrium concentration (mmol L^{-1}), q_e is the equilibrium adsorption capacity of the adsorbent (mmol kg^{-1}) and n is the constant illustrates the adsorption intensity (dimensionless), degree of non-linearity between solution concentration and adsorption.

The results suggest that lead ions adsorption on this biochar can be described by the Freundlich model (Fig. 5). The values of 1/n for was less than 1 (0.341, Table 3) suggest heterogeneity of the biochar surfaces, and the metal ions are favorably and intensively adsorbed by the biochar under the experimental conditions (Ahmad et al., 2012). As shown in Table (3), the K_F value was 234.7 mmol kg^{-1} with R^2 (0.916) while the maximum adsorption derived from Langmuir was 171.33 mmol kg^{-1} with R^2 (0.998). Comparing with the q_{max}, actual maximum adsorption, the value derived from Langmuir equation is much more reliable with the actual than of Freundlich equation. This may indicates that, lead ions adsorption could be better described by using Langmuir equation. Also, the large surface area of this SCBB might give the possibilities of the adsorbed ions to be on one not multi layers as Freundlich equation proposed.

3.5.3 Temkin Isotherm:

Temkin isotherm assumes that the heat of adsorption of the molecules in a layer decreases linearly due to adsorbent-adsorbate interactions and that adsorption is characterized by a uniform distribution of binding energies, up to some maximum binding energy (Shahmohammadi-Kalalagh et al. 2014). The adsorption experiment data of Pb (II) ions was analyzed by the linearized form of Temkin isotherm model as follows:

$$q_e = B \ln C_e + B \ln A \dots\dots\dots\dots\dots\dots.\dots. (7)$$

Where: $B = RT/b$, b is the Temkin constant related to heat of sorption (J mol^{-1}), R is the gas constant (8.314 J K^{-1} mol^{-1}), T is the absolute temperature (K) and A is the equilibrium binding

constant corresponding to the maximum binding energy (L g^{-1}).
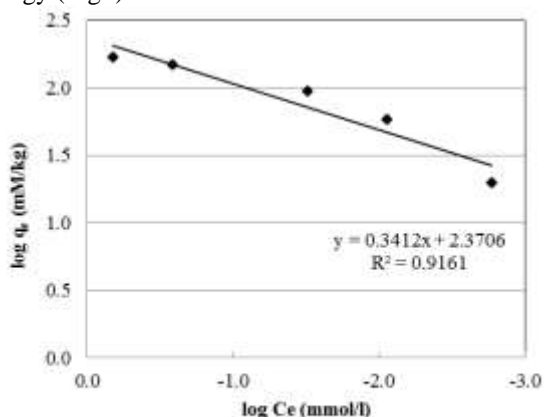
Figure 5. Freundlich isotherm plot for the adsorption of Pb^{+2} by SCBB at 25 C^o.

The plot of q$_e$ against ln C_e gives B (slope) and the intercept is (B ln A) as shown in Fig. 6. The Temkin parameters (Table 3) indicate that the model fits well with the experimental data of lead adsorption. Based on the linear regression values (R^2 > 0.99) which are considered as a measure of the goodness-of-fit of data, the experimental data of Pb adsorption isotherm followed the order, Temkin > Langmuir> Freundlich (Kim, et al., 2004). The monolayer adsorption capacity, according to the Langmuir isotherm, was found to be correlated with the actual maximum adsorption results. The fact that the assumptions of Temkin (adsorption is characterized by a uniform distribution of binding energies), and Langmuir (homogeneous distribution of active sites), the adsorption of lead ions can be described well with both of these isotherms.

3.5.4 Dubinin-Radushkevich Isotherm

This isotherm is generally used to distinguish between physical and chemical adsorption (Mohan, et al., 2007). It is given in the linearized form as:

ln q$_e$ = K$_{DR}$ ε^2 + ln q$_{max}$……………………………... (8)

Where:

q$_e$ the equilibrium adsorption capacity of the adsorbent (mmol kg^{-1}),

q$_{max}$ the maximum adsorption capacity (mmol kg^{-1}),

K$_{DR}$ the Dubinin-Radushkevich constant (mol^2 k^{-1}(J^2)$^{-1}$) and ε Polanyi potential given by,

ε = RT ln (1 + 1/C_e)………………………….. (9)

Where R is the gas constant (8.314×10^{-3} kJ K^{-1}mol^{-1}), T the absolute temperature in Kelvin and C_e the equilibrium concentration of metal ions (mmolL^{-1}). From (Eq. 8) the plot of ln q$_e$ against ε^2 gives a straight line with a slope of K$_{DR}$ and an intercept of q$_{max}$.
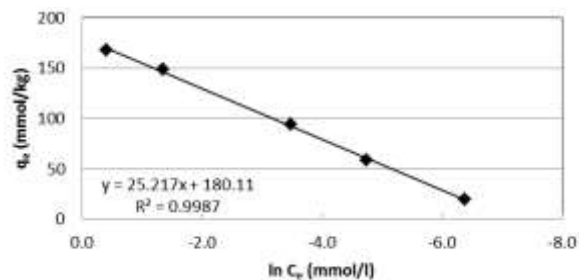
Figure 6. Temkin isotherm for lead adsorption by SCBB.

The Dubinin-Radushkevich isotherm also gives the mean energy of Pb (II) ions adsorption by the equation,

E = (-2 K$_{DR}$)$^{-1/2}$………………………………… (10)

If the E value is less than 8 kJ mol^{-1}, the process follows physical adsorption, and if the E value lies between 8 and 16 kJ mol^{-1}, the process follows chemical adsorption (Mohan et al. 2007). The Dubinin-Radushkevich isotherm model is shown in the (Figure 7) and its parameters are represented in the (Table 4). The mean energy of Pb (II) adsorption (E) was almost reached to 8 kJ/mol, which means lead adsorption on this biochar was mostly chemical in nature. Also, the maximum adsorption derived by using that equation represented the experimental value very well.

4. Adsorption kinetics:

A kinetics study of adsorption is desirable as it provides information about the mechanism of adsorption. The adsorption kinetic models are grouped into two classes and they are, adsorption reaction models: Pseudo First order model (Lagergren model), Pseudo Second order model and adsorption diffusion models: Intra-particle diffusion model and Boyd model (Debnath and Ghosh, 2008 and Kongsuwan et al, 2006).
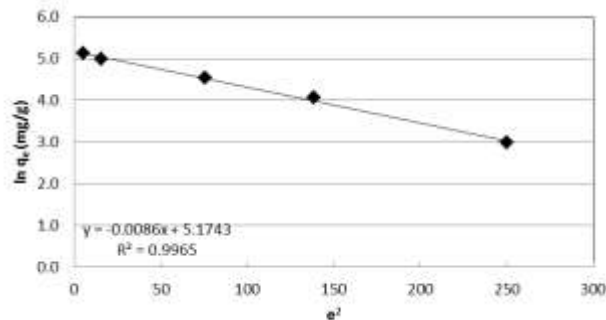
Figure 7. Dubinin-Radushkevich isotherm plot for the adsorption of Pb by SCBB.

4.1 Pseudo first order model:

Lagergren's first order rate equation has been most widely used for the adsorption of an adsorbate from an aqueous solution. The pseudo first order considers the rate of occupation of adsorption sites is directly proportional to the number of unoccupied sites. The pseudo first-order plot for the adsorption kinetics of Pb^{+2} to SCBB for various initial concentrations (0.1, 0.3, 0.5, 1.0 and 1.5 mmol L^{-1}) and adsorbent dose 5 g L^{-1}, at temperatures 25° C is given in Figure (8).

The linear form of this model was given by equation (11):

Table 4. Dubinin-Radushkevich Isotherm model parameter Pb sorption on SCBB at 25 C^o.

q max (mmol kg^{-1})	K_{Dr} (mol^2 k^{-1}(J^2)$^{-1}$)	E (KJ mol^{-1})	R^2
176.67	-0.009	7.63	0.9965

$$\ln (q_e - q_t) = \ln q_e - k_1.t\ldots\ldots\ldots.. (11)$$

Where: q_e and q_t are the adsorption capacities (mmol g^{-1}) at equilibrium and t time, respectively, and k_1 is the rate constant (Ho and Ofomaja, 2006).

The slope and intercept for the plots of log (q_e - q_t) versus t were used to determine the pseudo first-order rate constants, k_1 and q_e. They are given in Table (5) at different initial sorbent concentrations.

A good way to confirm that a reaction is of a particular order is to change only one parameter (e.g., initial concentration) and, in doing so, one should observe parallel kinetic plots resulting in similar apparent rate coefficients (Fendorf et al., 1993).

Figure (8) shows the first- order kinetic plots for Pb^{+2} adsorption at concentrations of 0.1, 0.3, 0.5, 1.0 and 1.5 mmol L^{-1} on SCBB. In this figure, at a constant temperature; $25C^0$, the slopes (apparent rate

coefficients) doesn't corresponded well (Table 5), confirming that the adsorption of Pb^{2+} on SCBB is not first-order type. For instance, at 0.1 and 1.5 mmol L^{-1}, Pb^{+2} adsorption resulted in apparent rate coefficients of 4.0 x 10^{-3} and 1.9 x 10^{-3} s^{-1}, with R^2 0.913 and 0.857 respectively.
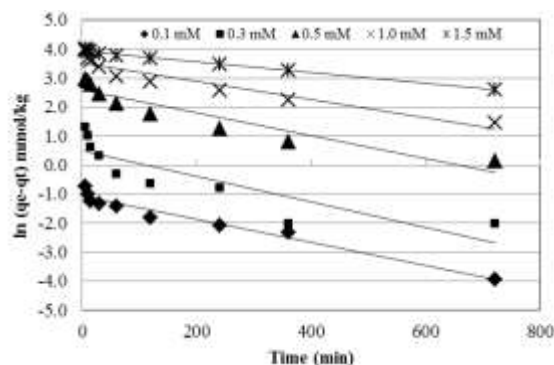
Figure 8. Pseudo First order kinetic plot for the adsorption of Pb by SCBB.

6-2 Pseudo second order model:

For adsorption system following the pseudo second kinetic model, the adsorbate was assumed to get adsorbed onto two surface type sites. Also this model considers that the rate of adsorption metal ions is based on the square of number of vacant sites on the adsorbent (Panday et al. 1985; Namasivayam and Kadirvelu 1997). The linear form this model was given in equation (12):

$$t/q_t = 1/(k_2 q_e^2) + t/q_e\ldots\ldots\ldots\ldots\ldots (12)$$

where q_e and q_t are the adsorption capacities (mmol kg^{-1}) at equilibrium and time t, respectively, and k_2 (kg mmol^{-1}min^{-1}) is the rate constant of pseudo-second order adsorption (Ho and Ofomaja, 2006).

Table 5. Pseudo First and second order kinetic parameters for the adsorption of Pb (II) by SCBB.

conc. (mmolL^{-1})	pseudo first order model			pseudo second order model			q$_e$ actual
	q$_e$ (mmolkg^{-1})	k_1	R^2	q$_e$ (mmolkg^{-1})	K_2	R^2	q$_e$ (mmolkg^{-1})
0.1	0.339	4.0*10^{-3}	0.913	19.646	70.59*10^{-3}	> 0.999	19.66
0.3	1.615	4.4*10^{-3}	0.796	58.14	19.46*10^{-2}	> 0.999	58.25
0.5	13.27	3.9*10^{-3}	0.950	94.34	1.92*10^{-3}	> 0.999	93.84
1.0	33.849	3.2*10^{-3}	0.840	149.254	0.58*10^{-3}	> 0.999	148.45
1.5	51.065	1.9*10^{-3}	0.857	166.67	0.24*10^{-3}	0.997	167.51

The pseudo second-order plot for the adsorption kinetic of lead (II) metal ions onto SCBB for various initial concentrations (0.1, 0.3, 0.5, 1.0 and 1.5 mmol L^{-1}), adsorbent dose 5 g L^{-1}, at temperatures 25^oC is given in Figure (9). The slope and intercept of plots of t/q_t versus t were used to calculate the pseudo second-order rate constants, k_2 and q_e at different initial

sorbent concentrations and shown in Figure (9). The second order rate constants k_2, the maximum adsorption constant, q_e values and correlation coefficients (R^2) were presented in Table (5). The nonlinear simulation plots were presented in Figure (9). The correlative coefficients of the second-order model are obviously higher than those of the first-

order model, indicating the second-order mode a comparatively suitable model to describe the lead ions adsorption process on SCBB.

The lead maximum adsorptions derived from the pseudo second-order model of the SCBB are given in Table (5). These values are very much consisted with the equilibrium maximum adsorption capacities (actual) Table (5). Previous studies of heavy metals kinetic on biochars gave the same behavior (Fendorf et al., 1993; Yahaya et al., 2011; Nwabanne and Igbokwe, 2011).

The calculated kinetic constants and their corresponding coefficient of determination (R^2) are given on Table (5). From these data, it was observed that except pseudo-second-order expression, no other model provided a better fit to the experimental kinetic data. The change in the adsorption capacity with time is found to fit the pseudo-second-order equation relationship which is based on the adsorption capacity of adsorbent phase. Because this equation is basically based on the adsorption capacity, the description of adsorption phenomenon suggests that the chemical reaction is rate controlling. It is indicated that these chemisorption systems involve vacancy forces through sharing or exchanging of electrons between the adsorbent and the solutes. This confirms perfectly the hypothesis based on two types of sites (Sparks and Suarez, 1991). In this study:

• The highly active sites, which react at the beginning time and are present in low concentrations on biochar;

• Less active sites, which react when the first sites are saturated, and are highly present at the surface of biochar.

6-3 Intra-Particle Diffusion Model:

The Weber–Morris intra particle diffusion model has often been used to determine if intra particle diffusion is the rate-limiting step (Thilagan et al., 2013). Accordingly the theory proposed by Weber and Morris is given in the equation (13):

$$q_t = K\, t^{1/2} + I \ldots\ldots\ldots\ldots\ldots\ldots\ldots\ldots (13)$$

Where: K is the intra-particle diffusion rate constant and I is the intercept. A plot of q_t against $t^{1/2}$ is drawn to examine the possibility of intra-particle diffusion as the rate determining step. The overall rate of adsorption can be described by the following three steps: (I) film or surface diffusion where the adsorbed ions is transported from the bulk solution to the external surface of adsorbent, (II) intra particle or pore diffusion, where adsorbed ions move into the interior of adsorbent particles, and (III) adsorption on the interior sites of the adsorbent. Since the adsorption step proceeded instantly, it is assumed that it does not influence the overall kinetics. The overall rate of adsorption process, therefore, will be controlled by either surface diffusion or intra particle diffusion.
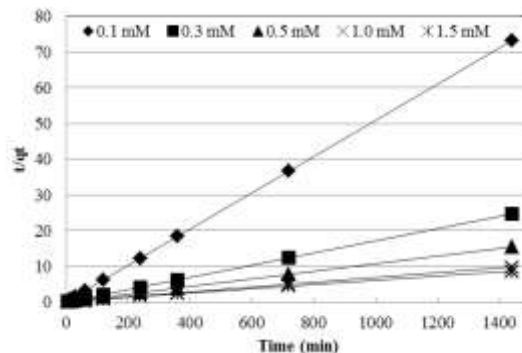
Figure 9. Pseudo second order kinetic plot for the adsorption of Pb (II) by SCBB.

According to this model, the plot of uptake, q_t, versus the square root of time ($t^{1/2}$) should be linear if intra particle diffusion is involved in the adsorption process and if these lines pass through the origin then intra-particle diffusion is the rate-controlling step. When the plots do not pass through the origin, it means, the intra-particle diffusion is not the only rate-limiting step, but also other kinetic models may control the rate of adsorption, all of which may be operating simultaneously (Ashtoukhy et al., 2008). The Weber–Morris intra particle diffusion model has often been used to determine if intra particle diffusion is the rate-limiting step (Sparks and Suarez 1991; Goswani and Ghosh, 2005).

In this study the adsorption of lead followed a multi-linear curves depending on the initial Pb^{+2} concentration and deviating from the origin, indicating more than one process affected the adsorption process, a two stage adsorption mechanism with first rapid and second slower has been observed. The first segment of the curves represented film diffusion and surface diffusion and the second segment represented intra-particle diffusion. Eq. (13) I_i is the intercept which are proportional to the extent of boundary layer thickness, Figure (10) and Table (6). The value of the intercept I_i in this second section provides information limiting step; similar phenomena have been observed by (Thilagan, et al 2013). The intra-particle diffusion, K_i, values were obtained from the slope of the straight-line portions of plot of q_t versus $t^{1/2}$ for various solutions concentrations. It was observed that intra-particle rate constant values (K_i) decreased with solution concentrations. Decreasing the concentration promoted the pore diffusion in adsorbent particles and resulted in an enhancement in the intra-particle diffusion rate. It is probable that a large number of ions diffuse into the pore before being adsorbed. It was observed that the straight lines did not pass through the origin and this further indicates that the intra-particle diffusion is not the only rate-controlling step.

Also, the diffusion coefficients for the intra-particle transport of ion within the pores of biochar particles have been calculated by employing the following equation (14):

$$D_i = 0.03 \, r^2 / t^{1/2} \ldots \ldots \ldots \ldots \ldots \ldots (14)$$

Where: D_i is the diffusion coefficients with the unit cm^2/s; $t^{1/2}$ is the time (s) for half-adsorption of the ion species and r is the average radius of the adsorbent particle in cm. The value of r (average radius) was calculated as 5×10^{-4} cm. In these calculations, it has been assumed that the solid phase consists of spherical particles. The diffusion coefficients varied from 0.9×10^{-11} to 1.3×10^{-11} cm^2/s with an increase of solution concentrations from 0.1 to 1.5 mmol L^{-1}. At lower concentration the attraction between the functional biochar-carbon groups and the metal ions get stronger. The values of the internal diffusion coefficient of Pb^{+2}, D_i, given in Table (6) fell well within the magnitudes reported in literature[35]

specifically for chemisorption system (10^{-5} to 10^{-13} cm^2/s). The parameters of intra-particle diffusion model for the adsorption of lead (II) ions by SCBB were estimated and given in the Table (6).
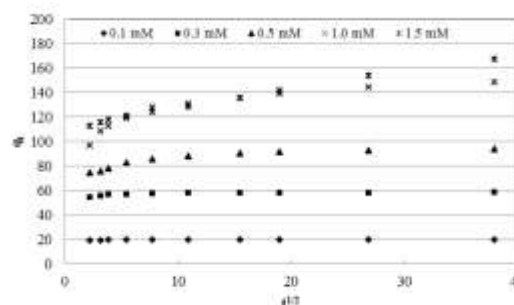
Figure 10. The Intra-particle diffusion kinetic plot for the adsorption of Pb (II) by SCBB.

Table 6. Intra-particle diffusion parameters and diffusion coefficient for the adsorption of Pb (II) by SCBB.

| initial conc. (mM) | intra particle diffusion parameter | | | | | | diffusion coefficient |
| | part 1 | | | part 2 | | | |
	K_1	I_1	R^2	K_2	I_2	R^2	D_i
0.1	0.1188	18.92	0.998	0.0089	19.37	0.912	5.00×10^{-11}
0.3	0.7139	53.20	0.908	0.0340	57.17	0.696	4.75×10^{-11}
0.5	2.1421	69.55	0.976	0.2525	85.39	0.833	4.31×10^{-11}
1.0	5.1614	89.63	0.928	0.6975	123.87	0.955	4.36×10^{-11}
1.5	2.6568	106.80	0.976	1.4678	112.95	0.997	4.84×10^{-11}

6-4 Boyd Model:

Multi-linear plots were obtained from the intra-particle diffusion model for the adsorption of lead (II) ions by SCBB, and in order to determine the actual rate controlling step involved in the adsorption process, the kinetic data have been analyzed using the model given by Boyd (Hu et al., 2011).
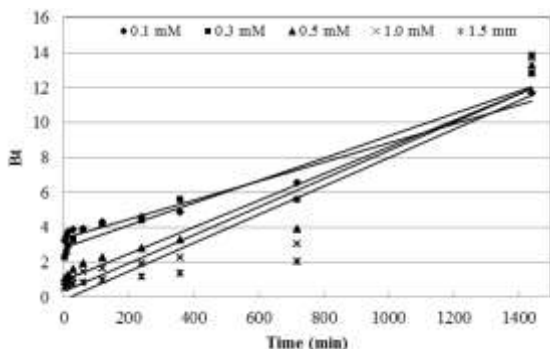
Figure 11. The Boyd plots for the adsorption of Pb (II) by SCBB.

The value of Bt plotted against time to configure the so-called Boyd plot (Hu et al., 2011). A straight line passing through origin is indicative of adsorption

processes governed by particle diffusion mechanism; otherwise they are governed by film diffusion (Hu et. al., 2011). The plots of Bt against t for the experimental data of various Pb^{2+} ions concentrations have been shown in figure (11). The plots of the lower ions concentrations very slightly deviated from the origin but at higher concentrations they reached to the origin. The plots in general were much linear which revealed that the intra-particle diffusion rather than film diffusion was the actual rate controlling step on the adsorption process of lead (II) ions by SCBB.

4. Conclusion

The high porous structure, intensive occurrence of surface functional groups, high surface area and great electro negativity enabled SCBB to be efficient biosorbent toward Pb^{2+} in aqueous solutions and remove more than 98% within the first 15 min. of removal reaction. The Pb^{2+} adsorption data were fitted to different isotherm model equations and Langmuir equation was found to be the best. Kinetic studies of adsorption revealed that the adsorption process followed pseudo second order kinetic model for Pb^{2+} on SCBB. The adsorption process was found to be controlled by surface and intra particle diffusion. Therefore, Sugar cane bagasse biochar is effective

adsorbent for the removal of Pb^{2+} from wastewater, since it is a low-cost, abundant and locally available.

References

1. Adepoju-Bello, A.A., Alabi, O.M., 2005. Heavy metals: A review. The Nig J Pharm. 37, 41-45.
2. Ahmad, M., Lee, S.S., Dou, X., Mohan, D., Sung, J.K., Yang, J.E. Ok, Y.S., 2012. Effects of pyrolysis temperature on soybean stover-and peanut shell derived biochar properties and TCE adsorption in water. Bioresour. Technol. 118, 536–544.
3. Al-Anber, Z., Al-Anber, M., 2008. Thermodynamics and Kinetic Studies of Iron (III) Adsorption by Olive Cake in a Batch System. J. Mex. Chem. Soc. 52 (2), 108-115.
4. Arami, M., Limaee, N.Y., Mahmoodi, N.M., Tabrizi, N.S., 2005. Removal of dyes from colored textile wastewater by orange peel adsorbent: equilibrium and kinetic studies, J. Colloid Interf. Sci. 288, 371–376.
5. Ashtoukhy, S.Z., Amin, N.K., Abdelwahab, O. 2008. Removal of lead (II) and copper (II) from aqueous solution using pomegranate peel as a new adsorbent. Desalination 223, 162 173.
6. Bakare-Odunola, M. T., 2005. Determination of some metallic impurities present in soft drinks marketed in Nigeria. *Nig. J. Of Pharm. Res.* 4 (1), 51-54.
7. Chen, B., Zhou, D., Zhu, L., 2008. Transitional Adsorption and Partition of Nonpolar and Polar Aromatic Contaminants by Biochars of Pine Needles with Different Pyrolytic Temperatures. Environ. Sci. Technol., 2008, 42 (14), pp 5137–5143.
8. Debnath, S., and Ghosh, U.C., 2008. Kinetics, isotherm and thermodynamics for Cr (III) and Cr (VI) adsorption from aqueous solutions by crystalline hydrous titanium oxide. Journal of chemical Thermodynamics 40: 67-77.
9. Dong, X., Ma, L.Q., Li, Y., 2011. Characteristics and mechanisms of hexavalent chromium removal by biochar from sugar beet tailing. J Hazard Mater., 190(1-3), 909-915.
10. Fendorf, S.E., Sparks, D.L., Franz, J.A., Camaioni, D.M., 1993. Electron paramagnetic resonance stopped-flow kinetic study of manganese (II) sorption-desorption on birnessite. Soil Sci. Soc. Am. J. 57, 57–62.
11. Gan, C., Liu, Y., Tan, X., Wang, S., Zeng, G., Zheng, B., Li, T., Jiang, Z., Liu, W., 2015. Effect of porous zinc–biochar nanocomposites on Cr (VI) adsorption from aqueous solution. RSC Adv., 5, 35107-35115.
12. Goswami S., Ghosh, U.C., 2005. Studies on adsorption behavior of Cr (VI) onto synthetic hydrous stannic oxide. Water SA 31, 597-602.
13. Gupta, V.K., Saini, V.K., Jain, N., 2005. Adsorption of As (III) from aqueous solutions by iron oxide-coated sand, J. Colloid Interf. Sci. 288, 55–60.
14. Ho, Y.S., Ofomaja, A.E., 2006. Pseudo-second-order model for lead ion sorption from aqueous solutions onto palm kernel fiber. J. Hazardous Materials 129, 137–142.
15. Hu, X.J., Wang, J.S., Liu, Y.G., Li, X., Zeng, G.M., Bao, Z.L., Zeng, X.X., Chen, A.W., Long, F., 2011. Adsorption of chromium (VI) by ethylenediamine modified crosslinked magnetic chitosan resin: isotherms, kinetics and thermodynamics. J. Hazard. Mater. 185, 306–314.
16. Inyang M., Gao, B., Pullammanappallil, P., Ding, W., Zimmerman, R.Z., 2010. Biochar from anaerobically digested sugarcane bagasse. Bioresource Technology 101, 8868–8872.
17. Khalid N., Ahmad, S., Kiani, S.N., Ahmed, J. 1998. Removal of Lead from Aqueous Solutions Using Rice Husk. Separation Sci. Technol. 33(15), 2349-2362.
18. Kim, Y., Kim, C., Choi, I., Rengraj, S., Yi, J., 2004. Arsenic removal using mesoporous alumina prepared via a templating method, Environ. Sci. Technol. 38, 924–931.
19. Kongsuwan, A., Patnukao, P., Pavasant, P., 2006. Removal of metal ion from synthetic waste water by activated carbon from Eucalyptus camaldulensis dehn bark. The 2nd International Conference on Sustainable Energy and Environment. Bangkok, Thailand:1-9.
20. Liang, B., Lehmann, J., Solomon, D., Kinyangi, J., Grossman, J., O'Neill, B., Skjemstad, J. O., Thies, J., Luizão, F. J., Petersen, J., Neves, E. G., 2006. Black carbon increases cation exchange capacity in soils. Soil Sci. Soc. Am. J. 70, 1719-1730.
21. Mahmoud, A.H., Saleh, M.E., Abdel-Salam, A.A., 2011. Effect of rice husk biochar on Cadmium in the immobilization in soil and uptake by wheat plant grown on lacustrine soil. Alex J. Agric. Res. 56: 117-125.
22. Mohan, D., Pittman, C.O., Bricka, M., Smith, F., Yancey, B., Mohammad, J., Steele, P.H., Alexandre-Franco, M.F., Gómez-Serrano, V., Gong, H., 2007. Sorption of arsenic, cadmium, and lead by chars produced from fast pyrolysis of wood and bark during bio oil production. J. Colloid and Interface Sci. 310 (1), 57–73.
23. Namasivayam C., Kadirvelu, K., 1997. Activated carbons prepared from coir pith by physical and

chemical activation methods, Biores. Technol. 62 (3), 123-127.

24. Nwabanne, J.T. Igbokwe, P.K.,. 2011. Copper (II) uptake by adsorption using Palmyra palm nut, Advances Applied Sci. Res. 2(6), 166-175.

25. Panday, K. K., Prasad, G., Singh, V.N., 1985. Copper (II) removal from aqueous solution by fly ash, Water Research, 19: 869-873.

26. Park, J.-H., Cho, Y.-S., Ok, S.-H., Kim, S.W., Kang, I.W. Coi, J-S. Heo, R.D. Delaune, D.-C. Sea., 2015. Competitive adsorption and selectivity sequence of heavy metals by chicken bone derived biochar: Batch and column experiment. Journal of Environmental Science and Health, Part A: Toxic/Hazardous Substances and Environ. Engin. 50(11), 1194-1204.

27. Putra, P.W., Kamari, A., Yusoff, M.N.S., Ishak, F.C., Mohamed, A., Hashim, N., Isa, M.I., 2014. Biosorption of Cu (II), Pb (II) and Zn (II) Ions from Aqueous Solutions Using Selected Waste Materials: Adsorption and Characterization Studies. J. Encapsulation Adsorption Sci. 4, 25-35.

28. Saleh, M.E., El-Refaey, A.A., Mahmoud, A.H. 2016. Effectiveness of sunflower seed husk biochar for removing copper ions from wastewater: a comparative study. Soil & Water Res., 11, 53-63.

29. Shahmohammadi-Kalalagh, Sh., Babazadeh, H., 2014. Isotherms for the sorption of zinc and copper onto kaolinite: comparison of various error functions. Int. J. Environ. Sci. Technol. 11, 111–118.

30. Shi, T., Jia, S., Chen, Y., Wen, Y., Du, C., Guo, H., Wang, Z., 2009. Adsorption of Pb (II), Cr (III), Cu (II), Cd (II) and Ni (II) onto a vanadium mine tailing from aqueous solution. J. Hazard. Mater. 169 (1–3), 838–846.

31. Sparks, D.L., Suarez, D.L., 1991. Rates of Soil Chemical Processes. Soil Sci. Soc. Am. Spec. Publ. 27 Soil Sci. Soc. Am., Madison, WI.

32. Sposito G., 1984. The Surface Chemistry of Soils. Oxford University Press, New York, 234 p.

33. Sumner, M. E., W. P. Miller, W.P., 1996. Cation exchange capacity and exchange coefficients. Pages 1201-1229. in D. L. Sparks, A. L. Page, and P. A. Helmke, editors, Methods of Soil Analysis. Part 3, Chemical Methods. Soil Science Society of America, Madison, Wisconsin, USA.

34. Thilagan, J., Gopalakrishnan, S., Kannadasan, T., 2013. A study on Adsorption of Copper (II) Ions in Aqueous Solution by Chitosan - Cellulose Beads Cross Linked by Formaldehyde. Inter. J. Pharmaceutical and Chemical Sci. 2(2), 2277-5005.

35. Uchimiya, M., Lima, I.M., Klasson, K.T., Chang, S., Wartelle, L.H., Rodgers, J.E., 2010. "Immobilization of heavy metal ions Cu (II), Cd (II), Ni (II), and Pb (II) by broiler litter-derived biochars in water and soil," J. Agric. Food Chem. 58(9), 5538–5544.

36. Yahaya, E.M., Latiff, M.F., Abustan, I., 2011. Adsorptive removal of Cu (II) using activated carbon prepared from rice husk by $ZnCl_2$ activation and subsequent gasification with CO_2. Inter. J. Engin. and Technol. 11(1), 164-168.

12/4/2017